Recombinant HIV envelope trimer selects for quaternary-dependent antibodies targeting the trimer apex

Devin Sok[a,b,c,d,1], Marit J. van Gils[e,1], Matthias Pauthner[a,b,c], Jean-Philippe Julien[b,c,f,g], Karen L. Saye-Francisco[a,b,c], Jessica Hsueh[a,b,c], Bryan Briney[a,b,c], Jeong Hyun Lee[b,c,f], Khoa M. Le[a,b,c], Peter S. Lee[f], Yuanzi Hua[b,c,f], Michael S. Seaman[h], John P. Moore[i], Andrew B. Ward[b,c,f], Ian A. Wilson[b,c,f,j], Rogier W. Sanders[e,i,2], and Dennis R. Burton[a,b,c,k,2]

[a]Department of Immunology and Microbial Science, [b]International AIDS Vaccine Initiative Neutralizing Antibody Center, [c]Center for HIV/AIDS Vaccine Immunology and Immunogen Discovery, [f]Department of Integrative Structural and Computational Biology, and [j]Skaggs Institute for Chemical Biology, The Scripps Research Institute, La Jolla, CA 92037; [d]International AIDS Vaccine Initiative, New York, NY 10038; [e]Laboratory of Experimental Virology, Department of Medical Microbiology, Center for Infection and Immunity Amsterdam, Academic Medical Center, University of Amsterdam, 1105 AZ Amsterdam, The Netherlands; [g]Program in Molecular Structure and Function, The Hospital for Sick Children Research Institute and Departments of Biochemistry and Immunology, University of Toronto, Toronto, Ontario, M5G 0A4 Canada; [h]Beth Israel Deaconess Medical Center, Boston, MA 02215; [i]Department of Microbiology and Immunology, Weill Medical College of Cornell University, New York, NY 10021; and [k]Ragon Institute of Massachusetts General Hospital, Massachusetts Institute of Technology and Harvard University, Boston, MA 02142

Edited by Beatrice H. Hahn, University of Pennsylvania, Philadelphia, PA, and approved October 31, 2014 (received for review August 21, 2014)

Broadly neutralizing antibodies (bnAbs) targeting the trimer apex of HIV envelope are favored candidates for vaccine design and immunotherapy because of their great neutralization breadth and potency. However, methods of isolating bnAbs against this site have been limited by the quaternary nature of the epitope region. Here we report the use of a recombinant HIV envelope trimer, BG505 SOSIP.664 gp140, as an affinity reagent to isolate quaternary-dependent bnAbs from the peripheral blood mononuclear cells of a chronically infected donor. The newly isolated bnAbs, named "PGDM1400–1412," show a wide range of neutralization breadth and potency. One of these variants, PGDM1400, is exceptionally broad and potent with cross-clade neutralization coverage of 83% at a median IC_{50} of 0.003 μg/mL. Overall, our results highlight the utility of BG505 SOSIP.664 gp140 as a tool for the isolation of quaternary-dependent antibodies and reveal a mosaic of antibody responses against the trimer apex within a clonal family.

HIV | broadly neutralizing antibodies | BG505 SOSIP | B cell | vaccine

Multiple methods have been developed to isolate HIV broadly neutralizing antibodies (bnAbs) (1–12). Hybridoma and phage display techniques were used to isolate the first generation of bnAbs including b12, 2F5, 2G12, 4E10, and Z13 (13–20). These antibodies exhibit a range of neutralization breadth against primary isolates from 30 to 90% but have moderate neutralization potency (median IC_{50} of ∼2–4 μg/mL). Access to infected donors who have high serum titers of bnAbs (21, 22) and the availability of newer approaches for isolating human mAbs have recently enabled the discovery of a new generation of more potent bnAbs (1–4, 6–8).

One of the newer approaches involves the sorting and activation of large numbers of memory B cells using cytokine-secreting feeder cells and the subsequent high-throughput screening of supernatants for neutralization. This method led to the identification and characterization of the first of the new generation of bnAbs, PG9 and PG16 (1), and since then has revealed several sites of vulnerability to bnAb recognition on HIV envelope (Env) (1–4, 6, 7). An alternative method of bnAb isolation involves the use of soluble Env molecules or scaffold proteins as baits to select single IgG^+ memory B cells of interest by cell sorting (6, 8, 9, 23, 24). However, soluble baits have not been successful in isolating antibody responses targeting quaternary epitopes, including the trimer-apex site surrounding the N160 glycan, because the protein constructs used to date have not properly mimicked native Env trimers. To address this problem, GFP-labeled 293T cells that express cell-surface Env, called "GFP-$293T^{BaL}$ cells," were used recently to isolate antibodies 3BC176 and 3BC315 (10, 25). These antibodies do not bind soluble monomeric gp120 but do bind Env trimer, demonstrating the utility of the approach, but the method was reported to be less efficient than the use of soluble protein baits (10, 25).

The favorable antigenic profile of the soluble BG505 SOSIP.664 gp140 trimer opens the possibility of its use for isolating quaternary-specific antibodies by single-cell sorting (26). To this end, we used BG505 SOSIP.664 gp140 to select for memory B cells from a donor from whom we previously had isolated the trimer-specific bnAbs PGT141–145 (3, 21). (For naming of PGT and PGDM bnAbs, please see *SI Materials and Methods*, *Antibody Nomenclature*.) We describe the isolation of previously unidentified somatic variants that are highly divergent from PGT145 and display a range of neutralization breadth and potency, with some being broader and more potent than the previously described PGT145 family members. Overall, the results reveal a mosaic of antibody responses against the trimer-apex site of vulnerability that have important

Significance

Despite the high antigenic diversity of the HIV envelope trimer (Env), broadly neutralizing antibodies (bnAbs) have identified conserved regions that serve as targets for vaccine design. One of these regions is located at the apex of Env and is expressed fully only in the context of the correctly folded trimer. This work describes the isolation of bnAbs that target this region using a recombinant native-like Env trimer as an affinity reagent to sort specific antibody-producing cells. Characterization of these antibodies reveals a highly diverse antibody response against the trimer apex and provides molecular information that will be useful in the design of immunogens to elicit bnAbs to this region of Env.

Author contributions: D.S., M.J.v.G., and D.R.B. designed research; D.S., M.J.v.G., M.P., J.-P.J., K.L.S.-F., J.H., J.H.L., K.M.L., P.S.L., Y.H., and M.S.S. performed research; D.S., M.J.v.G., J.P.M., A.B.W., and R.W.S. contributed new reagents/analytic tools; D.S., M.J.v.G., M.P., J.-P.J., B.B., J.H.L., I.A.W., and D.R.B. analyzed data; D.S., J.-P.J., and D.R.B. wrote the paper.

The authors declare no conflict of interest.

This article is a PNAS Direct Submission.

Data deposition: The sequences reported in this paper have been deposited in the GenBank database (accession nos. KP006370–KP006382 for heavy-chain sequences and KP006383–KP006395 for kappa-chain sequences). The atomic coordinates have been deposited in the Protein Data Bank, www.pdb.org (PDB ID code 4RQQ).

[1]D.S. and M.J.v.G. contributed equally to this work.

[2]To whom correspondence may be addressed. Email: rws2002@med.cornell.edu or burton@scripps.edu.

This article contains supporting information online at www.pnas.org/lookup/suppl/doi:10.1073/pnas.1415789111/-/DCSupplemental.

implications for immunogen design in general and for the future optimization of BG505 SOSIP.664 and related native-like trimers as vaccine candidates.

Results

Isolation of PGT145 Antibody Variants by Single-Cell Sorting. A variant of the BG505 SOSIP.664 gp140 trimer (26) bearing an Avitag sequence at the C terminus (BG505 SOSIP.664-AviB) was designed for site-specific biotinylation and subsequent conjugation to streptavidin-fluorophores. After confirming that antigenicity was not affected following biotinylation (Fig. S1), we used the BG505 SOSIP.664-AviB protein as bait to capture antigen-specific memory B cells from the peripheral blood mononuclear cells (PBMCs) of International AIDS Vaccine Initiative (IAVI) Protocol G donor 84, who is the elite neutralizer from whom the bnAbs PGT141–145 were isolated (3). The PBMCs were from the same time point used for isolation of PGT141–145. As for previously established methods (6, 8), we first excluded unwanted cell populations ($CD3^-/CD8^-/CD14^-$) followed by positive selection for IgG memory B cells ($CD19^+/CD20^+/IgG^+/IgM^-/IgD^-$). The memory population was sorted simultaneously for binding to BG505 SOSIP.664-AviB and lack of binding to biotinylated monomeric JR-CSF gp120 (JR-CSF gp120-AviB) (Fig. 1*A*). JR-CSF gp120 was included as a negative bait to select against antibodies binding nonfunctional trimers or monomers and was used in place of monomeric BG505 gp120 because this latter construct has been shown to bind to some quaternary trimer-apex–preferring antibodies, specifically PG9, to some degree (26). The cells of interest were singly sorted into lysis buffer, and mRNA was reverse transcribed and amplified by single-cell PCR to generate IgG heavy- and light-chain V genes (Table S1) (6, 27).

On average, one vial containing 10 million PBMCs yielded ~100 cells that bound to BG505 SOSIP.664-AviB but not to JR-CSF gp120-AviB. From two vials, we were able to obtain a total of 62 (31% recovery) heavy- and 158 (83% recovery) kappa-chain sequences, respectively (Fig. 1*B*). As shown in Fig. 1*B*, our sorting strategy strongly enriched for B cells that closely mimic PGT141–145 (42% of the isolated heavy-chain repertoire) in that they have extraordinarily long heavy chain complementary determining region 3 (CDRH3) of 33–34-aa CDRH3s and a mutation frequency of 21–27% from the V_H1-8 germline gene and 11–22% from the V_K2-28 germline gene (Fig. 1 *C* and *D* and Fig. S2). Although we also were able to isolate antibodies deriving from other germline genes, we chose to focus exclusively on those from the V_H1-8 gene with long CDRH3s.

Although we noted considerable enrichment for PGT141–145–like heavy- and light-chain sequences, we chose to clone and characterize only those sequences for which we were able to amplify a heavy- and light-chain pair. Thus, from 26 heavy-chain and 35 light-chain sequences, we obtained 13 somatic variants of the PGT145 antibody family that we have named "PGDM1400–1412" (Fig. S2). The previously unidentified variants are highly divergent from the previously isolated PGT141–145 antibodies; they are only 49–67% similar by amino acid sequence (Fig. S3) but nevertheless are members of this family as judged by gene use, CDRH3 length, and CDRH3 sequence (Fig. S2). Interestingly, the somatic variants PGDM1403–1407 and PGDM1409–1412 appear to have developed insertions and deletions that are not present in the other somatic variants (Fig. S2). The sequences segregate into distinct clusters based on the overall sequence identity (Fig. S3), and this clustering also is evident when represented as phylogenetic trees for both heavy chain (Fig. 2*A*) and light chain (Fig. 2*B*). To corroborate our findings, we were able to identify similar sequences for both heavy- and light-chain variants in a previously published next-generation sequencing dataset from the same donor (Fig. S4) (28).

New Somatic Variants from the PGT145 Antibody Family Vary in Their Neutralization Breadth and Potency. Next, the somatic variants PGDM1400–1406 were tested on a cross-clade 77-pseudovirus panel. The neutralization breadths and median IC_{50} values are presented by clade (Fig. 2*C* and Fig. S5). PG9 and the somatic variants PGT145 and PGT143 were included for comparison. Strikingly, despite sharing similar long CDRH3s and mutation frequencies, the variants display a wide range of both neutralization breadth (from 83–6% coverage; the IC_{50} cutoff was 2 μg/mL because of low production of some variants) and potency (from 0.003–0.173 μg/mL in median IC_{50}). These results highlight the enormous range of neutralization breadth and potency that can be observed in a single family of related nAbs from a single donor.

Somatic Variant PGDM1400 Is Broader and More Potent than Previously Reported bnAbs. Among the somatic variants characterized, the bnAb PGDM1400 stood out as having particularly broad and exceptionally potent neutralization activity. For a better comparison with previously described bnAbs, we measured neutralization breadth and potency on a 106-virus panel (Fig. S5) and calculated neutralization breadth at different IC_{50} cut-offs (Fig. 3*A*). These analyses confirmed that PGDM1400 is exceptionally potent; its median IC_{50} of 0.003 μg/mL is markedly superior to PGT121 (3), PGT128 (3), or PGT151 (11, 12), which are among the most potent bnAbs described to date (Fig. 3*A*). Furthermore, PGDM1400 also possesses high neutralization breadth, with 83% coverage (Fig. 3*A*). In addition, the combined neutralization coverage of PGDM1400 plus PGT121 reaches an extremely high neutralization breadth and potency, with 98% breadth at a median IC_{50} of 0.007 μg/mL, demonstrating the protective potential of a vaccine designed to elicit antibodies against two epitopes (Fig. 3*A*). Finally, given the incomplete neutralization noted for other trimer-dependent antibodies such as PGT151 and PG9, we evaluated the maximum percent neutralization (MPN) of PGDM1400 in comparison with PGT121, PGT151, PG9, and 12A12. The results show that PGDM1400 exhibits complete neutralization for more viruses than PGT151, and its MPN levels are comparable to those of PGT121 (Fig. S6).

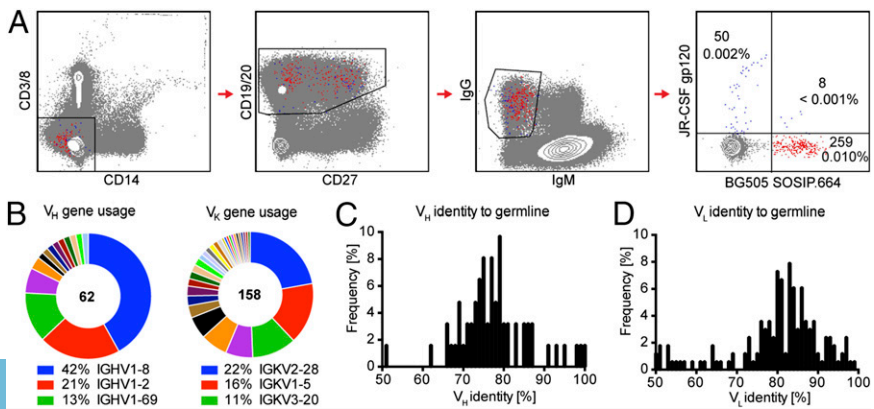

Fig. 1. BG505 SOSIP.664-AviB selects memory B cells expressing bnAbs from the PBMCs of the PGT141–145 donor. (*A*) PBMCs from the PGT141–145 donor were sorted using BG505 SOSIP.664-AviB and JR-CSF gp120-AviB. Events that are BG505 SOSIP.664-AviB$^+$ are shown in red, and events that are JR-CSF gp120-AviB$^+$ positive are shown in blue. (*B*, *Left*) A total of 62 productive heavy-chain sequences were obtained, with a large enrichment of the PGT145 antibody gene family V_H1-8. (*Right*) A total of 158 productive light-chain sequences were obtained, with a large enrichment for the PGT145 antibody gene family V_K2-28. (*C*) The heavy-chain sequences that were obtained are heavily mutated, with the majority having a mutation frequency of 20–30% from the inferred germ line. (*D*) The light chains also are mutated, with the majority having a mutation frequency of 10–20% from the inferred germ line.

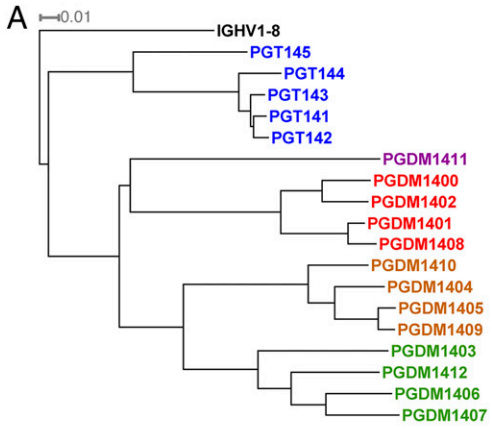

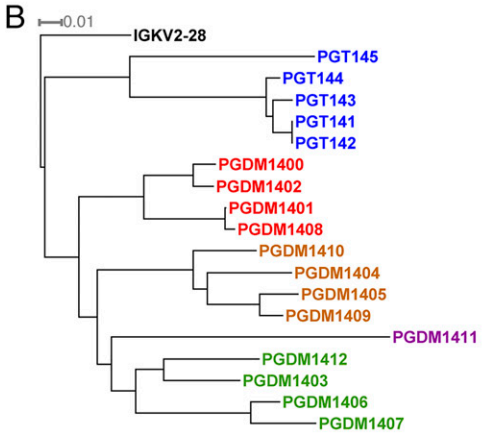

C

Clade	n	PGDM1400	PGDM1401	PGDM1403	PGDM1404	PGDM1405	PGDM1406	PG9	PGT143	PGT145
B	11	73%	64%	0%	9%	0%	0%	45%	45%	64%
B (T/F)	6	50%	33%	0%	0%	0%	0%	67%	33%	33%
C	13	85%	69%	31%	31%	31%	8%	85%	54%	54%
C (T/F)	8	88%	63%	50%	25%	38%	25%	88%	38%	63%
BC	6	100%	83%	100%	67%	33%	17%	100%	50%	100%
A	4	100%	75%	50%	50%	50%	0%	100%	50%	75%
A (T/F)	1	100%	100%	100%	100%	100%	100%	100%	100%	100%
CRF02_AG	6	100%	83%	67%	50%	17%	0%	83%	17%	33%
CRF01_AE	10	100%	70%	40%	60%	10%	0%	80%	70%	100%
CRF01_AE (T/F)	2	100%	0%	0%	0%	0%	0%	100%	0%	0%
G, D, CD, AC	10	70%	60%	30%	60%	30%	0%	90%	30%	60%
Total	**77**	**83%**	**65%**	**36%**	**38%**	**22%**	**6%**	**81%**	**44%**	**64%**
% Neutralization breadth		100%	80%	60%	40%	20%	0%			

Clade	n	PGDM1400	PGDM1401	PGDM1403	PGDM1404	PGDM1405	PGDM1406	PG9	PGT143	PGT145
B	11	0.550	0.017	NA	2.00	NA	NA	0.097	0.054	0.024
B (T/F)	6	1.65	0.102	NA	NA	NA	NA	0.723	0.274	0.051
C	13	0.001	0.005	0.102	1.00	0.006	2.00	0.064	0.242	0.042
C (T/F)	8	0.006	0.005	0.054	1.02	0.020	0.107	0.047	0.124	0.102
BC	6	0.001	0.001	0.022	1.00	0.002	0.021	0.049	0.005	0.097
A	4	0.001	0.001	0.023	0.003	0.003	NA	0.014	0.165	0.990
A (T/F)	1	0.002	0.008	0.023	0.009	0.162	0.819	0.023	0.023	0.028
CRF02_AG	6	0.016	0.015	0.013	0.044	0.006	NA	0.082	0.022	0.177
CRF01_AE	10	0.003	0.004	0.158	1.05	0.009	NA	0.079	0.070	0.055
CRF01_AE (T/F)	2	1.01	NA	NA	NA	NA	NA	1.00	NA	NA
G, D, CD, AC	10	0.003	0.003	0.093	1.00	0.009	NA	0.212	0.032	0.047
Total	**77**	**0.003**	**0.005**	**0.041**	**0.044**	**0.006**	**0.173**	**0.074**	**0.040**	**0.042**
Median IC_{50} (μg/mL)		1.00	0.100	0.010	0.001					

Fig. 2. Newly selected PGDM somatic variants display a range of neutralization breadth and potencies. (*A*) Heavy-chain phylogenetic tree of newly isolated somatic variants rooted at the V_H1-8 germline gene. The somatic variants cluster separately from the PGT141–145 antibodies and form four clusters that are distinct from the PGT141–145 cluster. (*B*) Kappa-chain phylogenetic tree of isolated somatic variants rooted at the V_K2-28 germline gene. The newly isolated somatic variants cluster separately from the PGT141–145 antibodies and match the clusters formed by the heavy-chain sequences shown in *A*. Phylogenetic trees were generated using Clustal Omega (43). (*C*) Percent neutralization breadth (*Upper*) and median IC_{50} values (*Lower*) of somatic variants PGDM1400–1406 against a 77-virus panel are listed by clade and colored according to the key. PG9 and the previously reported somatic variants PGT143 and PGT145 are listed for comparison. Somatic variants PGDM1402 and PGDM1407–PGDM1412 were not included because of low antibody yield.

We next wanted to compare possible structural differences between PGDM1400 and the previously isolated somatic variant PGT145 (3, 29). The structure of the PGDM1400 fragment antigen binding (Fab) determined at 3.1-Å resolution revealed that the 34-residue CDRH3 protrudes ∼25 Å above the other residues and adopts an extended β-hairpin conformation similar to that of the CDRH3 of PGT145 (Fig. 3*B* and Table S2) (29). CDR loops L1 and H2 appear to play a critical role in stabilizing the base of the elongated CDRH3 through an extensive network of H-bonding interactions (Fig. 3*B*). Sulfation is clearly observed in the electron density map for tyrosine at position 100F (Tys100F) (Fig. 3*B*). Unlike PGT145, which has two sulfated tyrosines exposed to solvent at the tip of the β-hairpin, sulfated Tys100F in PGDM1400 makes salt-bridge interactions with Arg100A, evidently providing internal stability to the kinked β-hairpin structure (Fig. 3*B*). A major difference between PGDM1400 and PGT145 residues occurs at the tip of the CDRH3 in the 100G–100R residue range, where only two of 12 residues are identical. A triad of aspartic acid residues provides a highly anionic potential to the tip of the PGDM1400 CDRH3 (Fig. 3*C*), which likely interacts with cationic residues in the gp120 V1/V2, as seen for PG9 and PG16 (29, 30). The 2D-class averages of the PGDM1400 Fab–BG505 SOSIP gp140 trimer complex obtained by single-particle negative-stain electron microscopy revealed that only a single Fab is bound at the trimer apex and binds predominantly along the threefold axis, in contrast to the shallower binding angle described for PG9 (Fig. 3*D*). PGDM1400, like other trimer-apex–targeted bnAbs such as PG9 (31) and CAP256-VRC26 (2), therefore targets the Env trimer with a stoichiometry of 1. Uncovering the atomic details of this interaction will help explain why PGDM1400 has such exceptional neutralization potency and breadth.

Despite Differences in Neutralization Activity, Somatic Variants Recognize a Similar Epitope. Considering the range of neutralization breadth and potency and the large sequence divergence between these clusters of somatic variants, we next determined whether they all bound to the same Env region. First, we tested binding to BG505 SOSIP-AviB by ELISA and found that all the somatic variants bound with varying affinities and that this binding was sensitive to the presence of particular glycoforms (Fig. 4*A*). Strikingly, despite binding to BG505 SOSIP-AviB by ELISA (Fig. 4*A*) and to cell surface BG505 Env (Fig. S7), some of the somatic variants did not neutralize the pseudovirus (Fig. S7), suggesting that a subset of functional Env on virions may not be targeted by these somatic variants. To determine if the variants are still quaternary-specific, we then tested binding to monomeric gp120. With one exception, PGDM1401, the somatic variants failed to bind to monomeric BG505 gp120 derived from lysed virions (lv_gp120) (Fig. 4*A*) or made as a recombinant protein in 293F cells (r_gp120) (Fig. 4*A*). This trimer binding preference was corroborated further for other isolates (Fig. 4*B*). Hence, we conclude that the somatic variants, regardless of

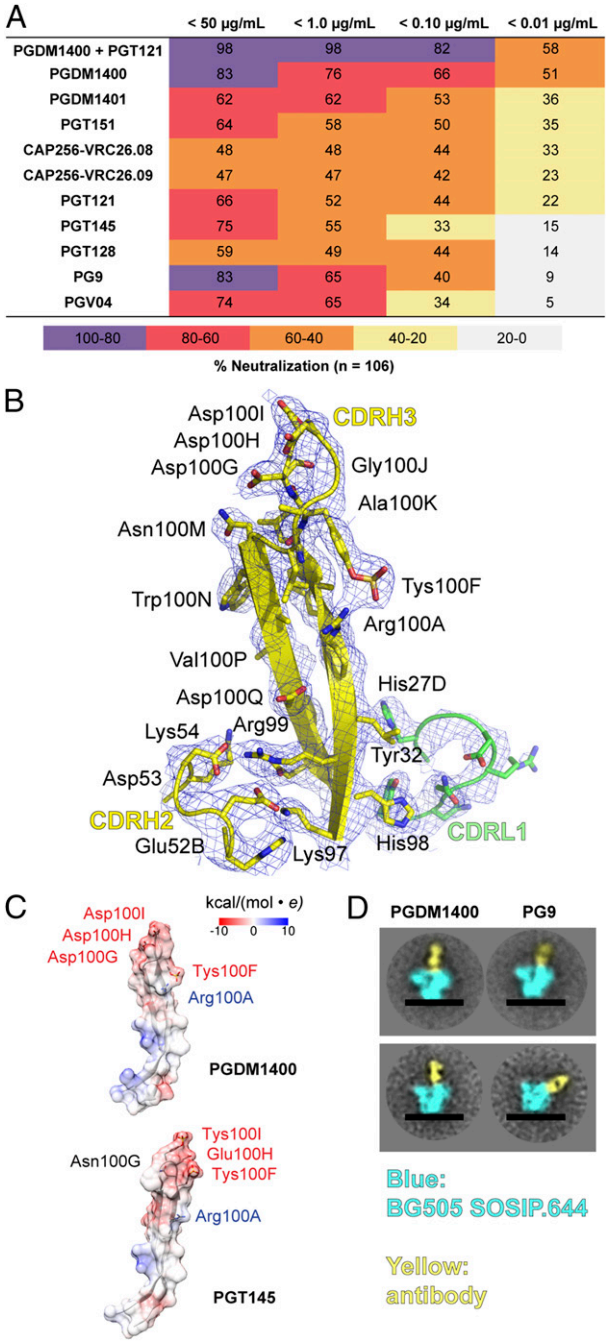

Fig. 3. PGDM1400 shows exceptional neutralization breadth and potency. (*A*) Percent neutralization breadth values on a cross-clade 106-virus panel at different IC_{50} cut-offs are listed for somatic variants PGDM1400 and PGDM1401 in comparison with previously reported bnAbs. The neutralization breadth and potency of the PGDM1400 + PGT121 combination was evaluated experimentally to show coverage obtained by targeting two different sites of vulnerability on Env. The color code for percent breadth values is given below the table. (*B*) Crystal structure of the PGDM1400 Fab. CDRH2, CDRH3 (yellow), and CDRL1 (green) are shown as a secondary structure cartoon with side chains depicted as sticks. The 2Fo-Fc electron density map is shown as a blue mesh contoured at 1.0 σ. The figure was made using Pymol (44). (*C*) Comparison between the elongated β-hairpin CDRH3s of PGDM1400 and PGT145. Key residues, including sulfated tyrosines, are shown as sticks. The transparent surface is colored as electrostatic potential according to Coulomb's law in UCSF Chimera (45). The CDRH3 orientations result from the structures being aligned on the entire Fab. (*D*) Reference-free 2D class averages of negative-stain EM of PGDM1400 Fab in complex with BG505 SOSIP.664. PG9 Fab complexed with BG505 SOSIP.664 was included for comparison. The regions corresponding to the trimer and Fab are colored in blue and yellow, respectively.

neutralization breadth, have a strong or absolute preference for Env trimers over gp120 monomers.

To probe the epitopes of the somatic variants further, we performed competition ELISAs and confirmed that all the somatic variants competed strongly with one another, except for PGDM1406, which did not compete with any of the tested antibodies (Fig. 4*C*). It is possible that this antibody has a trimer-binding affinity that is too weak to compete with the other somatic variants (Fig. 4*A*). When the broadest and most potent somatic variants, PGDM1400 and PGDM1401, were tested against a wider range of bnAbs, they competed only with those targeting the trimer-apex glycan epitope (Fig. 4*C*). Finally, as described for PGT141–145, we confirmed that all the newly isolated somatic variants are dependent on the N160 glycan for neutralization and showed reduced potency or loss of neutralization against pseudoviruses produced in the presence of kifunensine (Fig. 4*D*). Hence the overall data pattern strongly suggests that all somatic variants bind to the trimer-apex glycan epitope despite differences in their neutralization activity. Because of their N-linked glycan dependency, we also tested these somatic variants for autoreactivity in an HEp2 assay (Fig. S8). With the exception of PGDM1401, none showed evidence of autoreactivity.

Binding Kinetics of Less Broadly Neutralizing Variants Are Different from Those of Broadly Neutralizing Variants. To test the possible explanations for the differences in neutralization observed between broadly neutralizing and non-broadly neutralizing variants, we performed kinetic binding experiments by Octet (Fig. 4*E* and Fig. S9). Despite differences in the neutralization of BG505 pseudovirus (Fig. S7), the results confirmed the binding of both broadly neutralizing (PGT145 and PGDM1400) and non-broadly neutralizing (PGDM1403) antibodies to the BG505 SOSIP.664-AviB construct (Fig. 4*E*). Interestingly, although these three antibodies show similar overall binding affinities, we measured a faster off-rate for PGDM1403 than for PGT145 and PGDM1400. These differences in binding kinetics may play a role in the differences observed in the neutralization of the BG505 isolate (32).

Discussion

bnAbs are critical for revealing sites of vulnerability on HIV Env, especially in the context of vaccine design. Indeed, a finite number of these sites has been identified, and it is becoming apparent that subtle differences in epitope recognition define an antibody's neutralization breadth and potency (33–36). The results outlined here present a clear example of fine epitope specificity for the trimer-apex glycan epitope with somatic variants deriving from a common ancestor that yield neutralizing antibodies with breadths that range from exceptional (PGDM1400, 83%) to very limited (PGDM1406, 6%). The neutralization properties of PGDM1400, especially in combination with PGT121, also highlight its potential for delivery as a therapeutic antibody.

We and others have shown positive correlations between the level of somatic hypermutation and breadth of neutralization in a number of cases (2, 37, 38). Strikingly, in this case, there is little correlation between the breadth of antibody neutralization and the degree of somatic hypermutation among the somatic variants described (Fig. 2 and Fig. S2). The two somatic variants PGDM1400 and PGDM1406, for example, show similar levels of mutation from germ line but demonstrably different neutralization profiles for breadth and potency. It would appear that they have undergone maturation along different pathways. The maturation of PGDM1400 toward great breadth of neutralization is understandable if the antibody is mutating in response to neutralization escape variants and maintains positive interactions with conserved regions while accommodating potentially obstructive variable regions (37). PGDM1406, on the other hand,

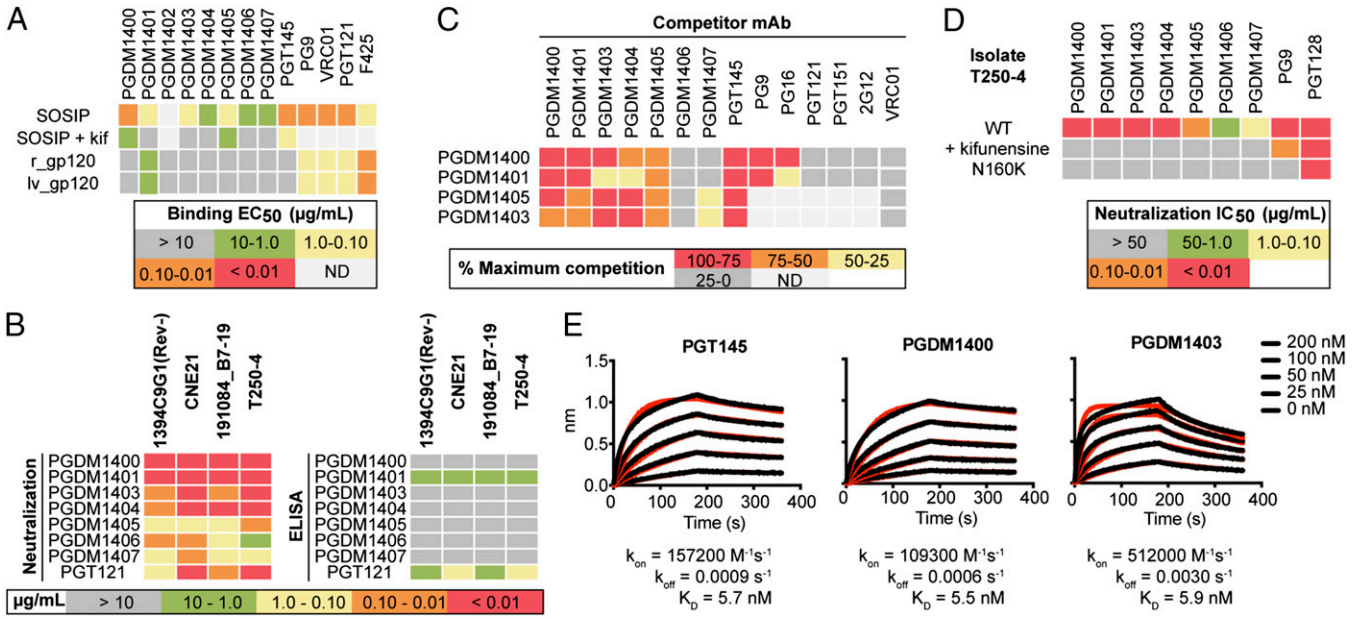

Fig. 4. Despite differences in neutralization, somatic variants bind to the same region on Env. (*A*) The somatic variants PGDM1400–1407 all bind to the BG505 SOSIP.664-AviB construct by ELISA. The same somatic variants do not bind or show reduced binding to BG505 SOSIP.664-AviB produced with kifunensine (SOSIP + kif) and, with the exception of PGDM1401, do not bind to r_gp120 or lv_gp120. The bnAbs PGT145, PG9, VRC01, PGT121, and F425 were included for comparison. Antibodies PGDM1408–1412 were not included because of low yield. (*B*) Viruses that are potently neutralized by the somatic variants PGDM1400–1406 were tested by ELISA for binding to corresponding gp120 monomers from lysed virions. Values represent neutralization IC_{50} or binding EC_{50} in micrograms per milliliter and are colored according to the key. PGDM1402 was excluded because of low yield. (*C*) The somatic variants PGDM1400, 1401, 1405, and 1403 were evaluated for competition with PGDM1400–1407 (PGDM1402 was excluded because of low yield) for binding to BG505 SOSIP.664 trimers in competition-binding ELISAs. Listed values are percent maximum competition as measured by ELISA and are colored according to the key. Antibodies that target the trimer apex (PGT145, PG9, and PG16) and those that do not (PGT121, PGT151, 2G12, and VRC01) were included for comparison. (*D*) Somatic variants PGDM1400–1407 (PGDM1402 was excluded because of low yield) were tested for neutralization against the T250-4 isolate, T250-4 N160K, and T250-4 + kifunensine. PG9 and PGT128 were included for comparison. (*E*) Antibodies PGT145, PGDM1400, and PGDM1403 were measured for binding to BG505 SOSIP.664-AviB by Octet. Black curves represent measured data points, and red curves represent best-fit lines following analysis.

likely diverged from PGDM1400 early, during affinity maturation in response to escape, and at some point responded to a particular virus in a way that lost breadth; this antigen must be distinct from classical HIV viral debris, because PGDM1406 remains quaternary-specific. Indeed, such a loss of neutralization breadth over the course of infection also has been described previously in the evolution of trimer-apex bnAbs (2).

Overall, these results suggest that antibodies take something of a "random walk" in response to natural infection that can lead either to very broad or very limited neutralization. Guiding antibody evolution in the right direction through vaccination may be very difficult through simple mimicry of natural infection: a more reductionist approach may be required in which clearly defined stages along the maturation pathway are targeted through the design of specific immunogens and proceed along a more carefully planned route.

The antibodies described here represent the first time, to our knowledge, that a soluble trimeric Env molecule (BG505 SOSIP.664 gp140) has been used to select quaternary-specific antibodies. Strikingly, antigen sorting with BG505 SOSIP.664 gp140 appears more effective than B-cell–culturing methods in recovering both higher numbers of bnAbs and bnAbs with greater potency. This difference likely reflects the limitations of each approach: antigen sorting is limited by affinity for antigen, whereas B-cell–culturing methods are limited by the capacity of memory B cells to secrete sufficient antibody concentrations for functional assays. Indeed, we have seen wide variability in the expression levels of these somatic variants as recombinant antibodies. Low-expression antibodies likely would be missed during screening following B-cell–culturing methods. In contrast, these same somatic variants can be recovered by antigen sorting provided they have sufficient affinity for the BG505 SOSIP.664 gp140 antigen bait. In addition to isolating new bnAbs to the trimer apex, BG505 SOSIP.664 gp140 potentially can be used to isolate bnAbs targeting other quaternary epitopes (11, 12, 39). Quaternary epitopes have been described as a major response among elite neutralizers of various cohorts, but 30–50% of these responses are not confirmed to target the trimer apex (21, 40, 41). The isolation of new bnAbs to fully define old and uncover new broadly neutralizing epitopes will continue to facilitate HIV vaccine design efforts.

Materials and Methods

Human Specimens. PBMCs were obtained from donor 84, an HIV-1–infected donor from the IAVI Protocol G cohort (21). All human samples were collected with written informed consent under clinical protocols approved by the Republic of Rwanda National Ethics Committee, the Emory University Institutional Review Board, the University of Zambia Research Ethics Committee, the Charing Cross Research Ethics Committee, the Uganda Virus Research Institute Science and Ethics Committee, the University of New South Wales Research Ethics Committee, St. Vincent's Hospital and Eastern Sydney Area Health Service, Kenyatta National Hospital Ethics and Research Committee, University of Cape Town Research Ethics Committee, the International Institutional Review Board, the Mahidol University Ethics Committee, the Walter Reed Army Institute of Research Institutional Review Board, and the Ivory Coast Comité National d'Éthique des Sciences de la Vie et de la Santé.

Single-Cell Sorting by Flow Cytometry. Sorting was performed as described previously (6, 27). In brief, donor PBMCs were stained with primary fluorophore-conjugated antibodies to human CD3, CD8, CD14, CD19, CD20, CD27, IgG, and IgM (BD Pharmingen) and 50 nM of BG505 SOSIP-AviB and 50 nM of JR-CSF gp120-AviB coupled to streptavidin- phycoerythrin (PE) and streptavidin-allophycocyanin (APC) (Life Technologies), respectively, in equimolar ratios. Staining was performed for 1 h at 4 °C in PBS with 1 mM EDTA and 1% FBS. In our gating strategy, we first excluded unwanted cell populations ($CD3^-/CD8^-/CD14^-$) followed by selection on BG505 SOSIP-Avi–specific memory B cells ($CD19^+/CD20^+/IgG^+/IgM^-$/BG505 SOSIP.$664^+$/JR-CSF $gp120^-$). Cells of interest

were single-cell sorted into 96-well plates containing lysis buffer on a BD FACSAria III sorter and were stored immediately at −80 °C (6, 27).

Pseudovirus Production and Neutralization Assays. To produce pseudoviruses, plasmids encoding Env were cotransfected with an Env-deficient genomic backbone plasmid (pSG3ΔEnv) in a 1:2 ratio with the transfection reagent Fugene 6 (Promega). Pseudoviruses were harvested 72 h posttransfection for use in neutralization assays. Neutralizing activity was assessed using a single round of replication pseudovirus assay and TZM-bl target cells, as described previously (3, 42). Kifunensine-treated pseudoviruses were produced by treating 293T cells with 25 μM kifunensine (TOSCO) on the day of transfection.

Detailed methods and the associated references can be found in *SI Materials and Methods*.

ACKNOWLEDGMENTS. This work was supported by the International AIDS Vaccine Initiative (IAVI) Neutralizing Antibody Consortium SFP1849 (D.R.B.); National Institutes of Health (NIH) Grants R01 AI033292 (to D.R.B.), R01 AI84817 (to I.A.W.), and R37 AI36082 (to J.P.M.); Center for HIV/AIDS Vaccine Immunology and Immunogen Discovery Grant UM1AI100663 (to D.R.B., I.A.W., and A.B.W.); and HIV Vaccine Research and Design Program Grant P01 AI82362 (to J.P.M., I.A.W., and A.B.W.). Funding also was provided by the NIH Interdisciplinary Training Program in Immunology 5T32AI007606-10 (D.S.); Dutch Aids Fonds Grant 2012041 and a European Molecular Biology Organization Application Short-Term Fellowship 260-2013 (to M.J.v.G.); Dutch Aids Fonds Grants 2009012 and 2011032 (to R.W.S.); a Vidi grant from the Netherlands Organization for Scientific Research (to R.W.S.); Starting Investigator Grant ERC-StG-2011-280829-SHEV from the European Research Council (to R.W.S.); and a Canadian Institutes of Health Research fellowship (to J.-P.J.). A portion of the neutralization experiments was done by the M.S. group (Beth Israel Deaconess Medical Center, Harvard Medical School), and that work was funded by Bill and Melinda Gates Foundation Grant 38619. The work of the IAVI is made possible by generous support from many donors, including the Bill and Melinda Gates Foundation; the Ministry of Foreign Affairs of Denmark; Irish Aid; the Ministry of Finance of Japan; the Ministry of Foreign Affairs of the Netherlands; the Norwegian Agency for Development Cooperation; the United Kingdom Department for International Development, and the US Agency for International Development (USAID). The full list of IAVI donors is available at www.iavi.org. This study was made possible by the generous support of the Bill and Melinda Gates Foundation Collaboration for AIDS Vaccine Discovery and the American people through USAID.

1. Walker LM, et al.; Protocol G Principal Investigators (2009) Broad and potent neutralizing antibodies from an African donor reveal a new HIV-1 vaccine target. *Science* 326(5950):285–289.
2. Doria-Rose NA, et al.; NISC Comparative Sequencing Program (2014) Developmental pathway for potent V1V2-directed HIV-neutralizing antibodies. *Nature* 509(7498):55–62.
3. Walker LM, et al.; Protocol G Principal Investigators (2011) Broad neutralization coverage of HIV by multiple highly potent antibodies. *Nature* 477(7365):466–470.
4. Bonsignori M, et al. (2011) Analysis of a clonal lineage of HIV-1 envelope V2/V3 conformational epitope-specific broadly neutralizing antibodies and their inferred unmutated common ancestors. *J Virol* 85(19):9998–10009.
5. Burton DR, et al. (2012) A blueprint for HIV vaccine discovery. *Cell Host Microbe* 12(4): 396–407.
6. Wu X, et al. (2010) Rational design of envelope identifies broadly neutralizing human monoclonal antibodies to HIV-1. *Science* 329(5993):856–861.
7. Huang J, et al. (2012) Broad and potent neutralization of HIV-1 by a gp41-specific human antibody. *Nature* 491(7424):406–412.
8. Scheid JF, et al. (2011) Sequence and structural convergence of broad and potent HIV antibodies that mimic CD4 binding. *Science* 333(6049):1633–1637.
9. Mouquet H, et al. (2012) Complex-type N-glycan recognition by potent broadly neutralizing HIV antibodies. *Proc Natl Acad Sci USA* 109(47):E3268–E3277.
10. Klein F, et al. (2012) Broad neutralization by a combination of antibodies recognizing the CD4 binding site and a new conformational epitope on the HIV-1 envelope protein. *J Exp Med* 209(8):1469–1479.
11. Falkowska E, et al. (2014) Broadly neutralizing HIV antibodies define a glycan-dependent epitope on the prefusion conformation of gp41 on cleaved envelope trimers. *Immunity* 40(5):657–668.
12. Blattner C, et al. (2014) Structural delineation of a quaternary, cleavage-dependent epitope at the gp41-gp120 interface on intact HIV-1 Env trimers. *Immunity* 40(5):669–680.
13. Burton DR, et al. (1994) Efficient neutralization of primary isolates of HIV-1 by a recombinant human monoclonal antibody. *Science* 266(5187):1024–1027.
14. Muster T, et al. (1994) Cross-neutralizing activity against divergent human immunodeficiency virus type 1 isolates induced by the gp41 sequence ELDKWAS. *J Virol* 68(6):4031–4034.
15. Burton DR, et al. (1991) A large array of human monoclonal antibodies to type 1 human immunodeficiency virus from combinatorial libraries of asymptomatic seropositive individuals. *Proc Natl Acad Sci USA* 88(22):10134–10137.
16. Zwick MB, et al. (2001) Broadly neutralizing antibodies targeted to the membrane-proximal external region of human immunodeficiency virus type 1 glycoprotein gp41. *J Virol* 75(22):10892–10905.
17. Barbas CF, 3rd, et al. (1992) Recombinant human Fab fragments neutralize human type 1 immunodeficiency virus in vitro. *Proc Natl Acad Sci USA* 89(19):9339–9343.
18. Trkola A, et al. (1996) Human monoclonal antibody 2G12 defines a distinctive neutralization epitope on the gp120 glycoprotein of human immunodeficiency virus type 1. *J Virol* 70(2):1100–1108.
19. Conley AJ, et al. (1994) Neutralization of divergent human immunodeficiency virus type 1 variants and primary isolates by IAM-41-2F5, an anti-gp41 human monoclonal antibody. *Proc Natl Acad Sci USA* 91(8):3348–3352.
20. Buchacher A, et al. (1994) Generation of human monoclonal antibodies against HIV-1 proteins; electrofusion and Epstein-Barr virus transformation for peripheral blood lymphocyte immortalization. *AIDS Res Hum Retroviruses* 10(4):359–369.
21. Simek MD, et al. (2009) Human immunodeficiency virus type 1 elite neutralizers: Individuals with broad and potent neutralizing activity identified by using a high-throughput neutralization assay together with an analytical selection algorithm. *J Virol* 83(14):7337–7348.
22. Gray ES, et al.; CAPRISA002 Study Team (2011) The neutralization breadth of HIV-1 develops incrementally over four years and is associated with CD4+ T cell decline and high viral load during acute infection. *J Virol* 85(10):4828–4840.
23. Wardemann H, et al. (2003) Predominant autoantibody production by early human B cell precursors. *Science* 301(5638):1374–1377.
24. Scheid JF, et al. (2009) Broad diversity of neutralizing antibodies isolated from memory B cells in HIV-infected individuals. *Nature* 458(7238):636–640.
25. Gaebler C, et al. (2013) Isolation of HIV-1-reactive antibodies using cell surface-expressed gp160Δc(BaL.). *J Immunol Methods* 397(1-2):47–54.
26. Sanders RW, et al. (2013) A next-generation cleaved, soluble HIV-1 Env Trimer, BG505 SOSIP.664 gp140, expresses multiple epitopes for broadly neutralizing but not non-neutralizing antibodies. *PLoS Pathog* 9(9):e1003618.
27. Tiller T, et al. (2008) Efficient generation of monoclonal antibodies from single human B cells by single cell RT-PCR and expression vector cloning. *J Immunol Methods* 329(1-2):112–124.
28. Zhu J, et al.; NISC Comparative Sequencing Program (2013) Mining the antibodyome for HIV-1-neutralizing antibodies with next-generation sequencing and phylogenetic pairing of heavy/light chains. *Proc Natl Acad Sci USA* 110(16):6470–6475.
29. McLellan JS, et al. (2011) Structure of HIV-1 gp120 V1/V2 domain with broadly neutralizing antibody PG9. *Nature* 480(7377):336–343.
30. Pancera M, et al. (2013) Structural basis for diverse N-glycan recognition by HIV-1-neutralizing V1-V2-directed antibody PG16. *Nat Struct Mol Biol* 20(7):804–813.
31. Julien J-P, et al. (2013) Asymmetric recognition of the HIV-1 trimer by broadly neutralizing antibody PG9. *Proc Natl Acad Sci USA* 110(11):4351–4356.
32. Yasmeen A, et al. (2014) Differential binding of neutralizing and non-neutralizing antibodies to native-like soluble HIV-1 Env trimers, uncleaved Env proteins, and monomeric subunits. *Retrovirology* 11:41.
33. Lyumkis D, et al. (2013) Cryo-EM structure of a fully glycosylated soluble cleaved HIV-1 envelope trimer. *Science* 342(6165):1484–1490.
34. Tran K, et al. (2014) Vaccine-elicited primate antibodies use a distinct approach to the HIV-1 primary receptor binding site informing vaccine redesign. *Proc Natl Acad Sci USA* 111(7):E738–E747.
35. Kong L, et al. (2013) Supersite of immune vulnerability on the glycosylated face of HIV-1 envelope glycoprotein gp120. *Nat Struct Mol Biol* 20(7):796–803.
36. Julien J-P, et al. (2013) Crystal structure of a soluble cleaved HIV-1 envelope trimer. *Science* 342(6165):1477–1483.
37. Sok D, et al. (2013) The effects of somatic hypermutation on neutralization and binding in the PGT121 family of broadly neutralizing HIV antibodies. *PLoS Pathog* 9(11):e1003754.
38. Liao H-X, et al.; NISC Comparative Sequencing Program (2013) Co-evolution of a broadly neutralizing HIV-1 antibody and founder virus. *Nature* 496(7446):469–476.
39. Scharf L, et al. (2014) Antibody 8ANC195 reveals a site of broad vulnerability on the HIV-1 envelope spike. *Cell Reports* 7(3):785–795.
40. Gray ES, et al.; CAPRISA 002 Study Team (2007) Neutralizing antibody responses in acute human immunodeficiency virus type 1 subtype C infection. *J Virol* 81(12): 6187–6196.
41. Walker LM, et al. (2010) A limited number of antibody specificities mediate broad and potent serum neutralization in selected HIV-1 infected individuals. *PLoS Pathog* 6(8): e1001028.
42. Li M, et al. (2005) Human immunodeficiency virus type 1 env clones from acute and early subtype B infections for standardized assessments of vaccine-elicited neutralizing antibodies. *J Virol* 79(16):10108–10125.
43. Sievers F, et al. (2011) Fast, scalable generation of high-quality protein multiple sequence alignments using Clustal Omega. *Mol Syst Biol* 7:539.
44. Schrodinger, LLC (2010) The PyMOL molecular graphics system, version 1.3r1. Available at www.pymol.org.
45. Pettersen EF, et al. (2004) UCSF Chimera—a visualization system for exploratory research and analysis. *J Comput Chem* 25(13):1605–1612.